J. Biochem. 2010;148(5):603–616 doi:10.1093/jb/mvq094

JB THE JOURNAL OF BIOCHEMISTRY

Molecular characterization of plant acidic α-mannosidase, a member of glycosylhydrolase family 38, involved in the turnover of *N*-glycans during tomato fruit ripening

Received July 14, 2010; accepted August 11, 2010; published online August 26, 2010

Md. Anowar Hossain[1,2], Ryohei Nakano[3], Kosuke Nakamura[1,4], Md. Tofazzal Hossain[2] and Yoshinobu Kimura[1,*]

[1]Department of Biofunctional Chemistry, Graduate School of Natural Science and Technology, Okayama University, Okayama 700-8530, Japan; [2]Department of Biochemistry and Molecular Biology, University of Rajshahi, Rajshahi 6205, Bangladesh; [3]Department of Plant Functions and Regulation, Graduate School of Natural Science and Technology, Okayama University, Okayama 700-8530; and [4]Kagome Research Institute, Kagome Co. Ltd, Nasu-gun, Tochigi 329-27, Japan

*Yoshinobu Kimura, Department of Biofunctional Chemistry, Graduate School of Natural Science and Technology, Okayama University, Tsushima-Naka 1-1-1, Okayama 700-8530, Japan. Tel.: +81 86 251 8296, Fax: +81 86 251 8388, email: yosh8mar@cc.okayama-u.ac.jp

The nucleotide sequence data has been submitted to the DDBJ/EMBL/GenBank databases under accession number GU434316.

It has been reported that acidic α-mannosidase activity increases during tomato fruit ripening, suggesting the turnover of *N*-glycoproteins is deeply associated with fruit ripening. As part of a study to reveal the relationship between the plant α-mannosidase activity and fruit maturation at the molecular level, we have already purified and characterized an α-mannosidase from tomato fruit (Hossain *et al.*, *Biosci. Biotechnol. Biochem.* 2009;73:140–146). In this article, we describe the identification and expression of the tomato acidic α-mannosidase gene using the yeast-expression system. The α-mannosidase-gene located at chomosome 6 is a 10 kb spanned containing 30 exons. The gene-encoded-protein is single polypeptide chain of 1,028 amino acids containing glycosyl hydrolase domain-38 with predicted molecular mass of 116 kDa. The recombinant enzyme showed maximum activity at pH 5.5, and was almost completely inhibited by both of 1-deoxymannojirimycin and swainsonine. The recombinant α-mannosidase, like the native enzyme, could cleave α1-2, 1-3 and 1-6 mannosidic linkage from both high-mannose and truncated complex-type *N*-glycans. A molecular 3D modelling shows that catalytically important residues of animal lysosomal α-mannosidase could be superimposed on those of tomato α-mannosidase, suggesting that active site conformation is highly conserved between plant acidic α-mannosidase and animal lysosomal α-mannosidase.

Keywords: acidic α-mannosidase/glycogene/*Lycopersicon esculentum*/plant *N*-glycan.

Abbreviations: bLAM, bovine lysosomal α-mannosidase; BMGY, buffered glycerol-complex medium; BMMY, buffered methanol-complex medium; dGMII, *Drosophila melanogaster* golgi α-mannosidase II; DMM, 1-deoxymannojirimycin; GlcNAc, *N*-acetyl-D-glucosamine; HEPES, 2-[4-2 (hydroxyl methyl)-1-piperazinyl] propane sulphonic acid; Man, D-mannose; Man-Le, α-mannosidase from *Lycopersicon esculentum*; MES, 2-morpholinoehtane sulphonic acid; Mn, (Man)nGlcNAc2-PA; MFX, Manβ1-4(Xylβ1-2)GlcNAcβ1-4GlcNAc(Fucα1-3)-PA; M2FX, Manα1-3Manβ1-4(Xylβ1-2)GlcNAcβ1-4GlcNAc(Fucα1-3)-PA; M3FX, Manα1-6(Manα1-3) Manβ1-4(Xylβ1-2)GlcNAcβ1-4GlcNAc(Fucα1-3)-PA; M5A, Manα1-6(Manα1-3)Manα1-6(Manα1-3)Manβ1-4GlcNAcβ1-4GlcNAc-PA; M6B, Manα1-6(Manα1-3) Manα1-6(Manα1-2Manα1-3)Manβ1-4GlcNAcβ1-4GlcNAc-PA; M7B, Manα1-6(Manα1-3)Manα1-6 (Manα1-2Manα1-2Manα1-3)Manβ1-4GlcNAcβ1-4GlcNAc-PA; M8A, Manα1-2Manα1-6(Manα1-3) Manα1-6(Manα1-2Manα1-2Manα1-3)Manβ1-4GlcNAcβ1-4GlcNAc-PA; M9A, Manα1-2Manα1-6 (Manα1-2Manα1-3)Manα1-6(Manα1-2Manα1-2Manα1-3)Manβ1-4GlcNAcβ1-4GlcNAc-PA; PA, pyridylamino; *p*NP-α-Man, *p*-nitro-phenol α-mannoside; RACE, rapid amplification of cDNA ends; rMan-Le, recombinant α-mannosidase from *Lycopersicon esculentum*; SF-HPLC, size fractionation HPLC; YPDS, yeast extract peptone dextrose medium.

Various α-mannosidases widely distributed in animals, plants and microorganisms, are involved in the biosynthesis and turnover of *N*-linked glycoproteins. α-mannosidases which involved in the *N*-glycan processing pathways and associated with endoplasmic reticulum associated protein degradation process have been well-studied in both animals and plants. On the other hand, lysosomal acidic α-mannosidases are involved in the degradation of *N*-glycans in animals and its deficiency causes a lysosomal storage disease called α-mannosidosis (*1*). Such kinds of vacuolar or cell-wall acidic α-mannosidases have been isolated and characterized from various plant sources, such as jack bean, rice, babaco, tomato, etc. (*2–5*). They could cleave mannose bonding with α-1,2, α-1,3 and α-1,6 linkages in high mannose and complex-type *N*-glycans. A number of evidences suggested that free *N*-glycans both high mannose-type and truncated complex-type were found to be increased in seeds

germination and fruits ripening stages. Free *N*-glycans were found as a significant fraction of the soluble oligosaccharide pool in tomato fruit pericarp (*6*). Also free *N*-glycans such as Man_3(Xyl)GlcNAc(Fuc) GlcNAc and Man_5GlcNAc were shown to stimulate tomato fruit ripening and had been postulated that free *N*-glycans could act as signalling molecule for plant growth-development and fruit ripening (*7*). Moreover, blocking of *N*-glycosylation with tunicamycin delayed tomato fruit ripening, suggests that *N*-glycoproteins may be important in ripening process (*8*).

We have found that free *N*-glycans levels are increased in developing plants such as seedling as well as tomato fruits ripening, suggesting that such free *N*-glycans might have a critical function for plant development or fruit-maturation (*9–12*). However, contrary to our expectation, it was found that the expression level of endo-β-*N*-acetylglucosaminidase (ENGase) did not vary significantly with the ripening process, suggesting that the increases in the amount of high-mannose type free *N*-glycans at the late-ripening stage was due to increase in the amount of endogenous substrates (misfolded glycoproteins) for ENGase or to a reduction in the degradation rate of free *N*-glycans (*13*). If such high-mannose type free *N*-glycans play as signalling molecules for fruit ripening, α-mannosidase also must play a critical role to regulate the putative physiological function of free *N*-glycan by rapid degradation. Recently, Meli *et al.* (*14*) have identified a gene of tomato *N*-glycan processing α-mannosidase accumulated in cell wall, and they proposed that the tomato α-mannosidase might play a critical role for tomato fruit ripening base on the suppression analysis of the tomato α-mannosidase-gene.

Glycoside hydrolysing (GH) enzymes have been classified into 85 families on the basis of sequence similarities. The family 38 (GH38) proteins are ~1,000 residues long and synthesized as a single polypeptide precursor that is posttranslationally cleaved into two to five polypeptide chains. This cleavage pattern appears to vary in different organisms (*4*, *15*, *16*). The native α-mannosidase isolated tomato fruits had two polypeptide chains (*5*). From the deduced amino acid sequence information, tomato acidic α-mannosidase can be classified in the class II α-mannosidase under glycosyl hydrolase family 38. Although many acidic α-mannosidases have been characterized from various plant sources, their physiological functions are still remained obscure for lacking of their genetic information. To elucidate the physiological role of vacuolar or cell wall acidic α-mannosidase involved in the plant development and fruit ripening, an isolation and identification of the plant acidic α-mannosidase-gene is prerequisite. Although similar tomato α-mannosidase gene has been identified and a physiological function has been postulated (*14*), detail substrate specificity, location of the gene in chromosome, and the information on structural biology of plant acidic α-mannosidase remain to be revealed. In our previous study, we described purification and characterization of an acidic α-mannosidase from tomato fruits, which was inhibited by two kinds of α-mannosidase-specific inhibitors (DMM and swainsonine) and preferred high-mannose or truncated type *N*-glycans having the chitobiosyl unit (GN2 type) to those having one GlcNAc residue (GN1 type) (*5*). Therefore, in this study, we describe cDNA expression and molecular characterization of acidic α-mannosidase from tomato fruit using *Pichia pasotris* as expression system. The substrate specificity of rMan-Le was same as that of native enzyme which suggested that it could hydrolysed α1-2, 1-3 and 1-6 α-mannosidic linkages in both the truncated plant complex-type or high-mannose type *N*-glycans.

Moreover, we have generated a molecular three-dimensional (3D) model from the deuced amino acid sequence information using SWISS-MODEL web server by homology modelling programme. It shows that the amino acid residues located at the active site of tomato α-mannosidase are conserved and superimposed with the Cα atom of bLAM, suggesting that active site conformation of tomato α-mannosidase is very similar to that of bLAM.

Materials and Methods

Materials

Mature red tomato (*Lycopersicon esculentum* mill. Cv Momotaro) fruits were collected from the Research Institute, Kagome Co. Ltd, Tochigi, Japan. An Asahipak NH2P-50-4E column (0.46 × 25 cm) was purchased from Showa Denko (Tokyo). TSK-Gel G3000SWXL (0.78 × 30 cm) was from Tosoh (Tokyo, Japan). *p*NP-α-Man, DMM and swainsonine were from Sigma Co. (St Louis, USA). Authentic PA-Sugar chains, M9A, M8A, M7B, M6B, M5A, GNM5, M3FX and GNM3FX were prepared as described in our previous papers (*17–19*). All synthetic oligonucleotide primers used in this study were obtained from Operon Biotechnologies, Tokyo, Japan. ANTI-FLAG®M2 affinity gel was purchased from Sigma-Aldrich Inc., St Louis, Missouri, USA.

RNA extraction and reverse transcription-polymerase chain reaction

Total RNA was extracted from mature red tomato by the hot borate method (*20*). Poly $(A)^+$ RNA was isolated using Oligotex-dT30 (Takara, Kyoto, Japan) in accordance with the manufacturer's protocol. The first strand of cDNAs synthesized by reverse transcription from 2 μg of poly $(A)^+$ RNA isolated from mature red tomato fruit were used as a template for RT–PCR with primers A and B (Table I). The gene-specific primers were designed on the basis of the nucleotide sequence information of tomato ESTs (SGN-U343973 and SGN-U327376). Reactions for the RT–PCR mentioned above were carried out for 35 cycles of 95°C for 1 min, 55°C for 1 min and 72°C for 3 min.

Amplification of full-length cDNA of α-mannosidase by RACE-PCR

To determine the full-length nucleotide sequence of putative α-mannosidase of *L. esculentum* (Man-Le), RACE-PCR was performed using a cDNA amplification kit (Marathon, Clontech, Palo Alto, CA, USA) according to the manufacturer's instructions. The 5′- and 3′-end fragments were amplified using gene-specific primers, C and E, respectively. Two other gene-specific primers, D and F were used for Nested-PCR for the amplification of the 5′- and 3′-end fragments (Table I). Each gene-specific primer was designed on the basis of the nucleotide sequence information of tomato ESTs (SGN-U343973 and SGN-U327376).

cDNA cloning and sequencing

The RACE-PCR products were ligated into a pGEM-T easy vector (Promega, USA) and transformed into *Escherichia coli* JM109

Table I. Oligonucleotide primers used for cloning of Man-Le gene.

Name		Nucleotide sequences	Uses
A	Man-F1-primer	ccgggaatgcagagcacagt	RT–PCR
B	Man-R1-primer	tcagggtggatggggaatga	RT–PCR
C	5′ RACE pr.Man-R1	gctctgcattcccgggctct	PCR/RACE-PCR amplification
D	5′ NEST pr.Man-R2	ttcctccaccaacgctggaaaa	PCR/NEST-PCR amplification
E	3′ RACE pr.Man-F1	tagaccaacctgctgctggaaa	PCR/RACE-PCR amplification
F	3′ RACE pr.Man-F2	tcttggagagggagcgaagtgg	PCR/NEST-PCR amplification
G	Man-F primer	cgttgtgggtagtggaagctaag	Amplification of full-length gene
H	Man-R primer	gtctcttcaacatcattataatta	Amplification of full-length gene
I	Seq.pr.Man-F1	caggtgcattccctcagaat	DNA sequencing
J	Seq.pr.Man-F2	catggttccggaatatggac	DNA sequencing
K	Seq.pr.Man-F3	ggtggaatcagcttcagcat	DNA sequencing
L	Seq.pr.Man-R1	aggagctaaagcccaaaggt	DNA sequencing
M	Seq.pr.Man-F4	tgcaaatggggcaaagttta	DNA sequencing
N	Seq.pr.Man-F5	gctgactgggatcttcaagtg	DNA sequencing
O	ClaI-FLAG-Man-F	atcgatg**gattacaaggacgacgacgacaag**atggtttacaatacatcacag	PCR amplification
P	NotI-Man-R	gcggccgctagagacatatgtgacttccaac	PCR amplification

Bold letters indicate Flag tag nucleotides and underlines indicate the cutting sites for restriction enzyme.

competent cells. After blue and white screening, the target cDNAs were sequenced with the M13 and various other sequencing primers (I–N, Table I) using a DNA sequencer (ABI Prism 3100-Avant Genetic Analyzer, Applied Biosystems, USA) according to the manufacturer's instructions. At least three colonies of each of the 5′- and 3′-end RACE-PCR fragments were sequenced for the correct determination of the cDNA sequence. To further confirm the sequence of full-length Man-Le, another pair of primer (G and H) were used to amplify the cDNA and cloned into a pGEM-T easy vector. The full-length cDNA was sequenced with the primers (I–N).

Construction of an expression plasmid for Man-Le

A hexa-His tag was fused with the open reading frame of the Man-Le gene at the C-terminal to facilitate the detection and purification of recombinant α-mannosidase. Another tag, Flag tag was fused with Man-Le gene at N-terminal after α-factor signal sequence of pPICZαC (Invitrogen, Carlsbad, CA, USA). The Man-Le cDNA was amplified by PCR using the oligonucleotide primers, 5′-ATCGATG**GATTACAAGGACGACGACGACAAG**ATGGTTTACAATACATCACAG-3′ (sense primer containing Flag tag with ATG start codon) and 5′-GCGGCCGCTAGAGACATATGTGACTTCCAAC-3′ (anti-sense primer). The Flag tag nucleotides were marked as bold letter. The *ClaI* and *NotI* restriction sites were designed into the sense and antisense primer, respectively. The primers used for PCR introduced *ClaI* and *NotI* restriction sites permitting the directional cloning of the amplified DNA in frame with the α-factor leader sequence in the pPICZαC expression vector. The PCR reaction was carried out using PrimeSTAR-HS DNA polymerase (Takara Bio Inc., Japan) for 30 cycles. The conditions for each cycle were as follows: denaturation at 98°C for 10 s, annealing at 55°C for 10 s, and extension at 72°C for 3.5 min. For cloning into the pGEM-T easy vector, the PCR products were subjected to phenol–ethanol precipitation and the adenine nucleotide was subsequently joined at the 3′-end using Takara *Ex Taq* DNA polymerase (Takara Bio Inc., Japan) at 72°C for 30 min. The PCR fragment of 3,006 bp was ligated into the pGEM-T easy vector and then transformed into *E. coli* JM109 cells with zeocin selection. The recombinant vector pGEM-T/Man-Le easy was isolated from *E. coli* cells and analysed cDNA sequence with various sequencing primers (Table I, I–N). The Man-Le cDNA insert obtained from the digestion of the recombinant pGEM-T/Man-Le easy vector with *PvuI*, *ClaI* and *NotI* was ligated into corresponding sites of pPICZα C (Fig. 4A). The recombinant vector, pPICZα C/Man-Le was transformed into *E. coli* JM109 in low-salt LB medium with zeocin. The correct orientation of the Man-Le insert was further confirmed with various sequencing primers (Table I). Unless otherwise stated, standard methods for the small-scale preparation of plasmids, digestion with restriction enzymes, ligation and transformation were used.

Transformation, screening and expression of Man-Le

Five to ten micrograms of pPICZα C/Man-Le DNA was isolated and linearized with *PmeI*. The digested DNA was ethanol precipitated and transformed into yeast *P. pastoris* GS115 strain using Pichia EasyComp kit (Invitrogen, Carlsbad, CA, USA) according to the manufacturer's instructions. Aliquots (150 µl) were spread on YPDS plates containing 100 µg/ml zeocin, and then the plates were incubated at 30°C for 4 days. The integration of Man-Le cDNA into the genome of *P. pastoris* was confirmed by PCR using 5′-AOX1 and 3′-AOX1 primers. *Pichia pastoris* GS115 albumin (Mut^S) and GS115/pPICZ/lacZ(Mut^+) were used as control strains for the determination of Mut phenotype. Seven colonies of transformants, which confirmed as Mut^+ phenotype, were grown in each of 25 ml of BMGY medium in 200 ml conical flask. The yeast culture was grown at 28°C in an incubator shaker at 250 rpm for ~24 h until the culture reached an $OD_{600} = 5.0$. The cultured yeast was harvested by centrifugation at 3000*g* for 5 min at room temperature. To induce expression of recombinant Man-Le, the pellet was re-suspended in 40 ml of BMMY medium and grown at 28°C with 250 rpm shaking for 5 days. Every 24 h, methanol (100%) was added to a final concentration of 0.5% to maintain induction, and at the same time, 1 ml of culture was collected for the expression detection and activity assay. Yeast growth media were prepared following the Pichia expression system protocol from Invitrogen (USA).

Extraction and purification of recombinant Man-Le

After confirming the period of the highest expression and activity of the recombinant Man-Le, the 120 h (5 days)-incubated Pichia culture medium was collected and centrifuged at 4,000*g* for 15 min in falcon tube (50 ml). Discarding the culture supernatant, Pichia cell pellet was collected for preparation of cell lysate. The cell lysate was prepared using Pichia breaking buffer (pH 7.4) according to manufacturer instruction. Then crude enzyme solution was applied onto an ANTI-FLAG®M2 affinity gel column for purification at 4°C according to manufacturer's instructions. The protein concentration was measured by measuring the absorbance at 280 nm with bovine serum albumin (BSA), as standard.

Assay system for α-mannosidase activity

Assay method for p-nitrophenyl α-D-mannopyranoside. The activity of rMan-Le was measured using *p*-nitrophenyl α-D-mannopyranoside (*p*NP-α-Man) as a synthetic substrate. The enzyme solution (20 µl) was added to 20 µl of *p*NP-α-Man (5 mM) in 50 µl of 0.1 M MES buffer, pH 6.0. After 1 h of incubation at 37°C, the reaction was stopped by adding 1.0 ml of 1.0 M glycine–NaOH buffer, pH 10.5. The released *p*-nitrophenol was measured by taking the absorbance at 420 nm. One unit of enzyme activity was defined as the amount of enzyme releasing 1 µmol of *p*-nitrophenol per min at 37°C.

Assay method for pyridylaminated N-glycans. A reaction mixture (70 µl) containing ~100 pmol PA-sugar chain M9A and 20 µl of enzyme in 0.1 M MES buffer (pH 5.5), was incubated at 37°C for 4 h. The enzymatic reaction was stopped by heating in the boiling water for 3 min. After centrifugation, an aliquot (30 µl) of the reaction mixture was analysed by size-fractionation (SF)-HPLC, as described in previous paper (*5*). The rate of hydrolysis (%) was

calculated from the following equation; hydrolysis (%) = 100−$A/B \times 100$, where A is area of the remaining substrate on the chromatogram, B is a sum of area of all PA-sugar chains on the chromatogram (PA-sugar chains produced and the remaining substrate).

SDS–polyacrylamide gel electrophoresis

The purified rMan-Le was analysed by SDS–PAGE (7.5% polyacrylamide) in 0.1 M Tris–glycine buffer using slab gel apparatus according to the method of Laemmli (*21*). Twenty microlitres of the supernatant was added to each lane of the gel. After electrophoresis, the gel was stained with Coomassie Brilliant Blue R-250 and de-stained by washing with a mixture of acetic acid–methanol–water (10:25:65, v/v/v). The marker proteins used for molecular weight determination were Precision Plus Protein^{TM} Standards (250, 150, 100, 75, and 50 kDa) (Bio-Rad).

Effects of pH and temperature on the activity of rMan-Le

The effects of pH on the activity of rMan-Le were determined using M9A and *p*NP-α-Man as substrates at various pH levels (3.0–8.0). The effects of temperature also were examined at various temperatures (20–80°C) followed by standard assay method described in the earlier section. The enzymatic activities were calculated as percent relative to the highest rMan-Le activity sample observed in this assay.

Effects of metal ions and inhibitors on the activity of rMan-Le

The effects of metal ions on the activity of rMan-Le were investigated using Fe^{2+}, Fe^{3+}, Mn^{2+}, Co^{2+}, Ca^{2+}, Zn^{2+}, Cu^{2+}, Mg^{2+} and EDTA at a concentration of 5 mM. The effects of two α-mannosidase specific inhibitors, swainsonine and DMM were also examined. After pre-incubation of various metal ions and inhibitors with purified rMan-Le separately in 0.1 M MES buffer, pH 5.5, the reaction mixtures were incubated with M9A substrate at 37°C for 6 h. Then remaining substrate and products after reaction were calculated as percent.

Substrate specificity of rMan-Le

Study of the substrate specificity of rMan-Le was carried out using authentic PA-sugar chains: M9A, M8A, M7B, M6B, M5A, GNM5, M2FX, M3FX and GNM3FX. PA-sugar chains were incubated with purified rMan-Le in 0.1 M MES buffer, pH 5.5, at 37°C for 2 h. The PA-sugar chains produced after rMan-Le digestion were analysed by SF-HPLC on a Shodex Asahipak NH2P-50-4E column (0.46 × 25 cm). The PA-sugar chain mixture was eluted by increasing the water content in water-acetonitrile from 20 to 80% linearly over 50 min at a flow rate of 0.7 ml/min. PA-sugar chains were detected with a Jasco FP-920 Intelligent Fluorescence detector (excitation at 310 nm, emission at 380 nm).

Bioinformatics analysis

The signal peptide was detected using Predisi (*PREDIction of Signal peptides*), Germany (http://www.predisi.de/). The theoretical molecular mass and an isoelectric point (pI) of Man-Le were determined by ExPASy Proteomics Server (http://www.expasy.ch/tools/pi_tool.html). PredictProtein (*22*) online software was used to identify the *N*-glycosylation sites in the deduced amino acid sequence of Man-Le (http://www.predictprotein.org/). The most conserved domains in the deduced amino acid sequence of Man-Le were identified by conserved domain database (CDD) search at the National Center for Biotechnology Information (NCBI) web server. The Man-Le amino acid sequence was compared with that of bLAM using on online multiple alignment programme, ClustalW2 (http://www.ebi.ac.uk/Tools/clustalw2/). To explore the Man-Le sequence neighbours or homologues, we used non-redundant sequence database at (NCBI) by BlastP search. The query sequence was amino acid sequence of Man-Le. The amino acid sequence homologues of Man-Le were completely aligned using ClustalX (2.0.6) programme. Finally, phylogenetic reconstruction of the sequences was carried out using distance/neighbour-joining programme, ClustalX (2.0.6) (*23*). The 3D structure of Man-Le was created by SWISS-MODEL automated protein structure homology-modelling server (http://swissmodel.expasy.org/) which accessible via the ExPASy web server or from the programme DeepView (Swiss Pdb-Viewer) (*24–26*). The quality of the modelled structure was assessed by the determination of DFire and QMEAN scores as well as PROMOTIF (*27–29*). Stereochemistry of the structure was also verified by the Whatif and Procheck programmes in the same server (*30*, *31*).

Results and Discussion

Cloning, sequencing and identification of Man-Le cDNA

We previously purified and characterized a α-mannosidase from mature red tomato fruits and determined the N-terminal sequences of two subunits (*5*). In this study, we used that N-terminal amino acid sequences for the silico analysis and identified two expressed sequence tags (ESTs), SGN-U343973 and SGN-U327376 as candidate ESTs in the Sol Genomic Network. On the basis of ESTs sequence information we designed two gene-specific primers, A and B from SGN-U343973 and SGN-U327376, respectively, for the RT–PCR amplification to detect the cDNA present in reverse transcription samples. The RT–PCR sample showed the 1,700 bp fragments on 1% agarose gel electrophoresis (data not shown). After purification, the amplified cDNA was subsequently cloned and sequenced. The sequence had 99% identities with the both EST sequences. Moreover, the RT sample and genomic DNA were also subjected to PCR amplification using another pair of primer (K and L) for obtaining short PCR products. The genomic DNA–PCR product size (1,850 bp) was larger than RT–PCR product (370 bp) suggested that genomic DNA contained much more introns in genomic DNA (data not shown). The presence of introns in Man-Le gene was also supported by the exon–intron organization (Fig. 2). To obtain the 5′- and 3′-end of cDNA, the 5′- and 3′-RACE-PCR and nested-PCR were performed using gene-specific primers (C–F). The amplified fragments were cloned into pGEM-T easy vector and determined the sequence of three clones. We used another pair of primer, G and H for the PCR amplification to obtain the full-length cDNA, which was found to be 3,361 bp. It was registered under the GenBank accession no. GU434316 (Fig. 1). The cDNA sequence found in our clones showed 99% identities with ESTs, SGN-U343973 and SGN-U327376. The size of the full-length cDNA was two times longer than that of the summation of two EST sequences. These results suggested that ESTs clones, SGN-U343973 and SGN-U327376, were the part of the Man-Le mRNA. The Man-Le mRNA had maximum identities found in NCBI BLAST nucleotide search with the mRNA sequences of *Ricinus communis* (77%, XM_002512794.1), *Populus trichocarpa* (76%, XM_002321039.1) and *Vitis vinifera* (76 %, XM_002276056.1).

Man-Le gene is organized in 30 exons

Nucleotide Blast search showed that Man-Le cDNA had 100% identities with *L. esculentum* genomic DNA, Bacterial Artificial chromosome (BAC) clone C06HBa0086B01 (GenBank: AC209509.1). Man-Le gene is located at the chromsome 6 of *L. esculentum*. The full-length of this BAC clone is 104,773 bp. The Man-Le gene spanned ~10 kb and consisted of

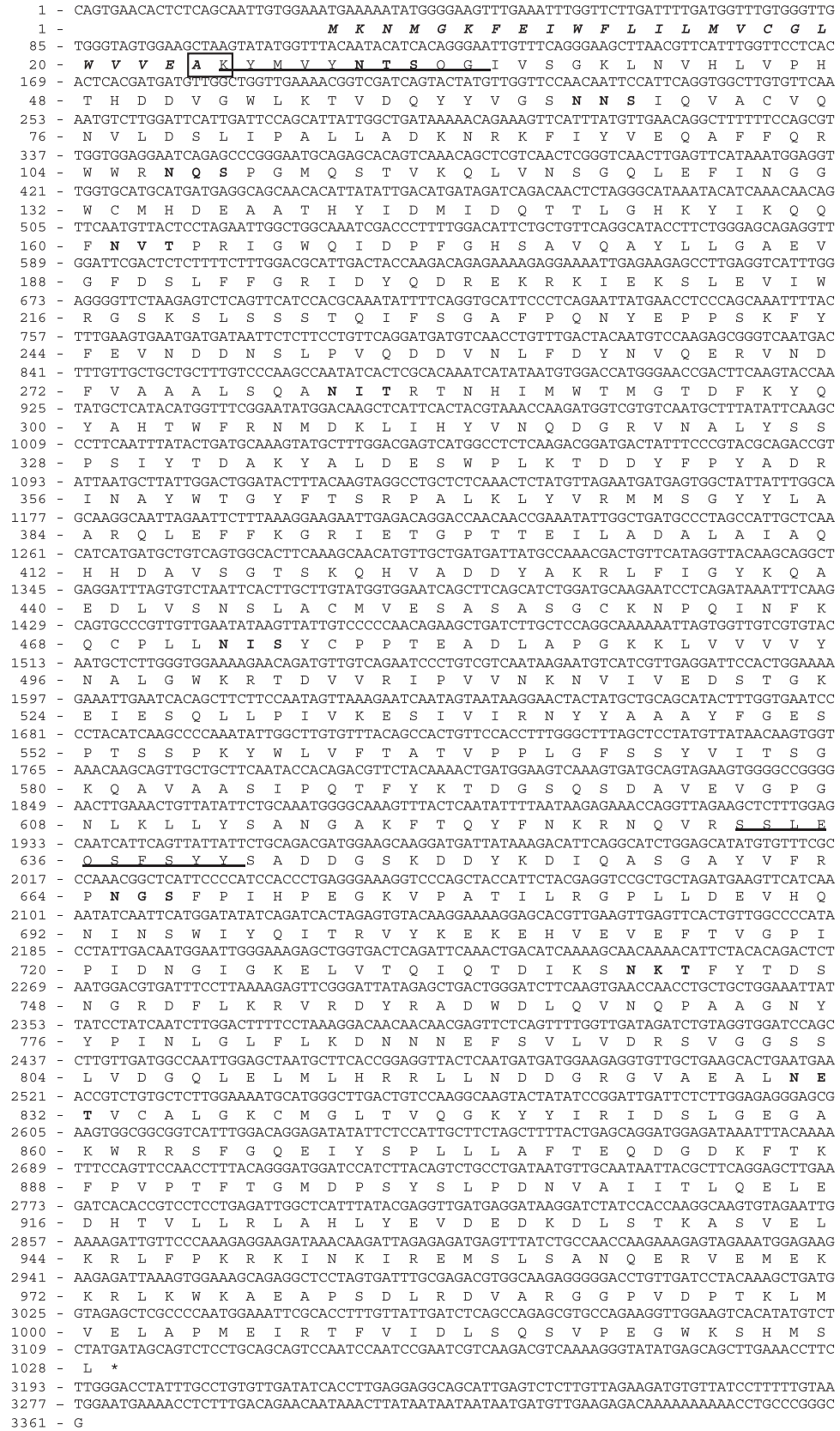

Fig. 1 Nucleotide and deduced amino acid sequence of Man-Le cDNA. The translated sequence of Man-Le Signal peptide includes a 24 amino acid signal peptide shown in italic bold letter. Signal peptide cleavage site is shown in box. The predicted nine *N*-glycosylation sites were indicated as bold letter. N-terminal sequences of large and small subunit of native Man-Le were marked as underlined.

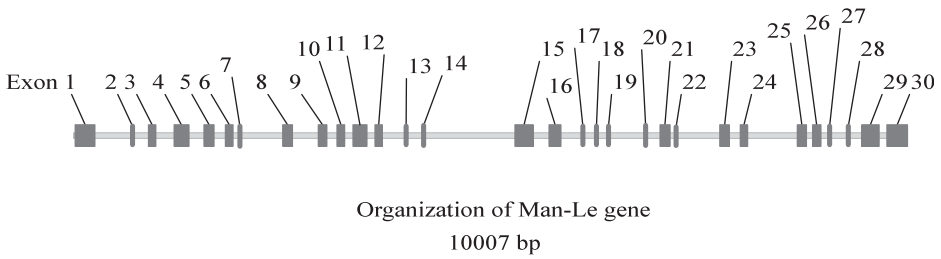

Fig. 2 An organization of Man-Le gene. The gene located at the chromosome 6 under BAC clone C06Hba0086B01.1 found in the GenBank is illustrated from 5′ (left) to 3′ (right). Exons 1–30 are indicated by gray boxes. Total length of the gene was 10,007 bp.

30 exons as well as 29 introns (Fig. 2). The first exon started at 26,091 bp and 30th exon ended at 36,097 bp.

Sequence analysis

A 3,084 bp open-reading frame (ORF) was obtained from the cDNA sequence isolated from tomato fruits. It coded for a polypeptide of 1,028 amino acid residues of which the first N-terminal 24 amino acid residues forms the signal sequence (Fig. 1). Earlier we identified the N-terminal amino acid sequence as 10 amino acids (KYMVYNTSQG) in the native tomato α-mannosidase. It is located at 25th to 35th position of deduced amino acid sequence (*5*). The observation was confirmed by using Signal p 3.0 server and Predisi (*PREDIction of Signal peptides*) which showed the existence of cleavage site between position 24 and 25: VEA-KY (Fig. 1). Therefore, the mature Man-Le is a single polypeptide containing 1,004 amino acid residues with a predicted molecular mass of 114 kDa and pI 6.19. A typical poly $(A)^+$ tail was found at the 3′ untranslated region. Further analysis showed that the deduced amino acid sequence contained the nine *N*-glycosylation sites. The position of predicted *N*-glycosylation sites were 30, 66, 107, 161, 281, 473, 665, 740 and 830 in the deduced amino acid sequence. The conserved domain database search programme in the NCBI web server showed three mostly conserved domains in the primary amino acid sequence of Man-Le. They are glycosyl hydrolase super family 38 N-terminal domain, α-mannosidase (middle domain) and glycosyl hydrolase super family 38 C-terminal domain (Fig. 3B). Therefore, these results demonstrated that Man-Le belongs to glycosyl hydrolase family 38. Sequence alignment showed amino acid identities of ~43% with bLAM. The important residues located at the active site of bLAM are fully conserved in the Man-Le polypeptide (Fig. 3A) suggests that the catalytic mechanism of Man-Le could be similar to that of bLAM.

Expression of Man-Le cDNA and purification of rMan-Le

Since native Man-Le N-terminal sequence started at position 25 in the deduced amino acid sequence of Man-Le we used cDNA sequence (3,006 bp) without signal peptide sequence for the construction of expression vector (Fig. 4A). The Man-Le cDNA amplified by PCR using the oligonucleotide primers, O and P, was cloned into the pPICZα C expression vector in frame with the α-factor leader sequence. The recombinant vector, pPICZα C/Man-Le was transformed into competent cells of *E. coli* JM109. The inserted DNA sequence was analysed and further confirmed by PCR amplification and sequence analysis. The recombinant plasmid, pPICZα C/Man-Le DNA isolated and linearized with *PmeI*, was used for transformation into *P. pastoris* GS115 strain with zeocin screening. A single colony of transformants expressing Mut^+ phenotype was grown in BMGY medium, and finally, expression was induced by methanol in BMMY medium. The resulting culture supernatant and cell lysate were analysed for α-mannosidase activity using *p*NP-α-Man as well as PA-sugar chain, M9A as substrates. While high enzyme activity was found in the *Pichia* cell lysate, only marginal activity could be detected in the culture supernatant (data not shown). In contrast, the cell lysate from *Pichia* with the expression vector pPICZα C (without Man-Le cDNA insert) had no α-mannosidase activity, indicating that endogenous α-mannosidase activity could not be detected in the Pichia extract used in this enzyme assay system. However, α-mannosidase activity could be detected in Pichia with the expression vector pPICZαC when both the amount of sample and incubation time was increased. For example, prolonged incubation time, such as over night incubation (16 h), showed the weak endogenous α-mannosidase activity against both type of substrates (data not shown). Our time-course study revealed that 120 h (5 days) was an optimum incubation time for maximizing the intracellular expression in Pichia cell after methanol-induction (data not shown) in BMMY media. We purified rMan-Le by anti-flag affinity column. SDS–PAGE of the purified proteins which was incubated at 50°C for 2 h, showed a major band at ~270 kDa and a minor protein bands at ~135 kDa (Fig. 4B). Two other aliquots both reducing and non-reducing conditions heated on boiling water for 3 min showed single band at ~135 kDa, suggesting that this major band might be dimer of rMan-Le associated with strong hydrophobic interaction that could be destroyed only at high temperature in the presence of SDS. The bLAM was also found to occur in dimeric form by similar strong hydrophobic interaction (*32*). The theoretical molecular mass of cloned cDNA-encoded polypeptide is 114 + 21 kDa from predicted nine Asn-linked oligosaccharides and two fusion tags. The apparent molecular mass seems to be good agreement with the theoretical molecular mass of glycosylated rMan-Le. Although the expression construct (pPICZαC) had the secretion

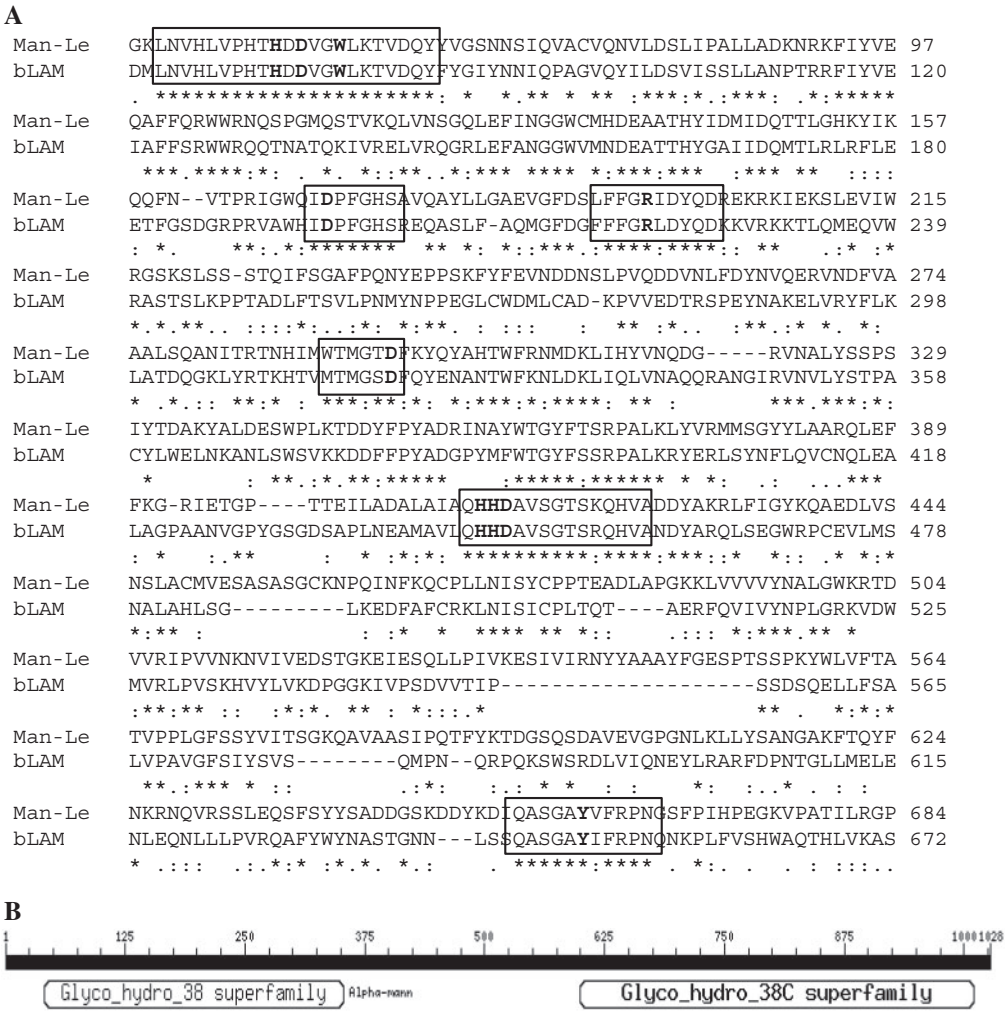

Fig. 3 Amino sequence alignment and conserved domains. (A) Alignment of Man-Le with Bovine lysosomal α-mannosidase (bLAM, accession no. Q29451) showed 43% identity and amino acids located around the active site marked as bold letter in boxes. Only highly conserved regions of both enzymes are shown (positions of amino acid for Man-Le and bLAM were 38–684 and 61–672, respectively). (B) The conserved domains were identified by conserved domain database (CDD) search programme in the NCBI web server. Glycosyl hydrolases super family 38 N-terminal domain (residue number: 41–353), alpha mannosidase, middle domain (residue number: 358–432) and glycosyl hydrolase super family 38 C-terminal domain (residue number: 599–110). '*' represents the conserved amino acid, ':' represents very similar amino acid, and '.' represents similar amino acid.

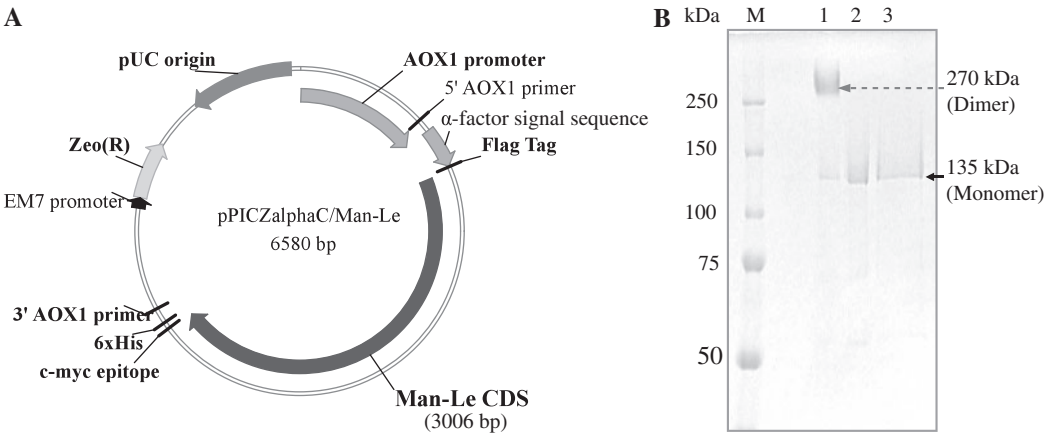

Fig. 4 Man-Le Expression vector construct and SDS–PAGE. (A) Man-Le expression construct. The Man-Le cDNA (3,006 bp) was expressed under AOX1 promoter with N-terminal Flag and C-terminal His tag. (B) Purity Flag-rMan-Le-$(His)_6$-fusion protein was checked by 7.5% acrylamide and stained with Coomassie brilliant blue R-250. Lane M, marker proteins; lane 1, purified flag-rMan-Le-$(His)_6$-fusion protein heated at 50°C for 2 h; lane 2, heated on boiling water for 3 min without β-mercaptoethanol; lane 3, heated on boiling water for 3 min with β-mercaptoethanol. Determination of molecular mass of purified flag-rMan-Le-$(His)_6$-fusion protein. The proteins used in the calculation of molecular masses were Precision Plus Protein™ Standards (BioRad): 250, 150, 100, 75 and 50 kDa. M1 and M2 are monomer and dimer of rMan-Le, respectively.

signal, rMan-Le protein could not be secreted into the media. At this moment, it is difficult to make a rational explanation why the rMan-Le protein could not be secreted into the media, but we speculate that it could be due to a proteolytic cleavage by an endogenous proteinase in the secretion signal sequence after the expression of Man-Le cDNA in Pichia cells. In this case, the apparent molecular mass would undergo very little change.

Effects of pH and temperature on the activity of rMan-Le

The effects of pH and temperature on the activity of rMan-Le were analysed using *p*NP-α-Man and PA-sugar chain, M9A as substrates. For synthetic the substrate, the rMan-Le showed optimum activity at pH 5.5–6.0 and the activity rapidly declined after pH 6.0 (Fig. 5A). Whereas for the natural substrate, an optimum activity was observed in between the pH 4.0 and 5.5, which reached its maximum level at pH 5.5. Although the optimum activity was found in the acidic region of pH, a little activity (8.6%) was retained at pH 8.0. This result suggests that Man-Le could reside in the acidic region of cell either cell wall or vacuole, although the optimum pH is slightly higher than those (pH 3.5–4.5) of other plant α-mannosidases (*2–4*, *33*, *34*), suggesting that physiological function of Man-Le may be different from those other plant acidic α-mannosidases [Jack bean enzyme (*2*) or rice enzyme (*3*)] working in the protein body or vacuole. The optimum temperature of rMan-Le for both synthetic and natural substrate was found to be at around 40–50°C (Fig. 5B), which was consistent with other α-mannosidases (*2–4*, *15*, *33*, *34*).

Effects of metal ions and inhibitors on the activity of rMan-Le

The effects of metal ions and inhibitor on the activity of rMan-Le were very similar to that of native Man-Le isolated from tomato fruits (*5*). When rMan-Le pre-incubated with various metal ions was incubated with M9A as substrate, most of the metal ions inhibited the α-mannosidase activity (Table II). Cu^{2+} partly inhibited the rMan-Le activity as found in *Ginko* α-mannosidase (*35*). For the control sample (without metal), no. of substrate (M9A) remaining after reaction and the final product was M4 whereas in the presence of Cu^{2+} only 5% substrate (M9A) was converted to product (M8). Many α-mannosidases reported so far required metal ions such as Zn^{2+}, Ca^{2+} for full enzymatic activity (*2*, *3*, *33*, *34*, *36*, *37*), whereas rMan-Le was inhibited some extent by both metals, suggesting that this tomato α-mannosidase is a novel acidic α-mannosidase in plant. Moreover, EDTA also weakly inhibited the activity like other metal ions. Thus there is a possibility that this enzyme required metal ions beside eight metals tested in this study. The activity was significantly inhibited by mannose specific inhibitor DMM and completely inhibited by swainsonine. Since Jack bean, rice and bLAMα-mannosidases are significantly inhibited by swainsonine but not DMM, the hydrolytic mechanism of Man-Le must be slightly different from other acidic α-mannosidases reported so far (*2*, *3*, *32*).

Substrate specificities

The substrate specificity of rMan-Le was analysed using various pyridylaminated *N*-glycans as substrates. The substrate specificity of rMan-Le is almost the same as that of native tomato α-mannosidase (*5*), and rMan-Le could hydrolyse α-mannosidic linkages in both high-mannose and truncated complex-type *N*-glycans (Fig. 6A). However, hybrid type structure (GNM5) or one of truncated complex type structures M2FX, showed resistance towards rMan-Le. Arabidopsis Golgi α-mannosidase II can easily hydrolyse α1-6 mannosidic linkage in $GlcNAc_1Man_5Xyl_1Fuc_1GlcNAc_2$-PA or $GlcNAc_1Man_5GlcNAc_2$-PA, and convert them to $GlcNAc_1Man_3Xyl_1Fuc_1GlcNAc_2$-PA or $GlcNAc_1Man_3GlcNAc_2$-PA,

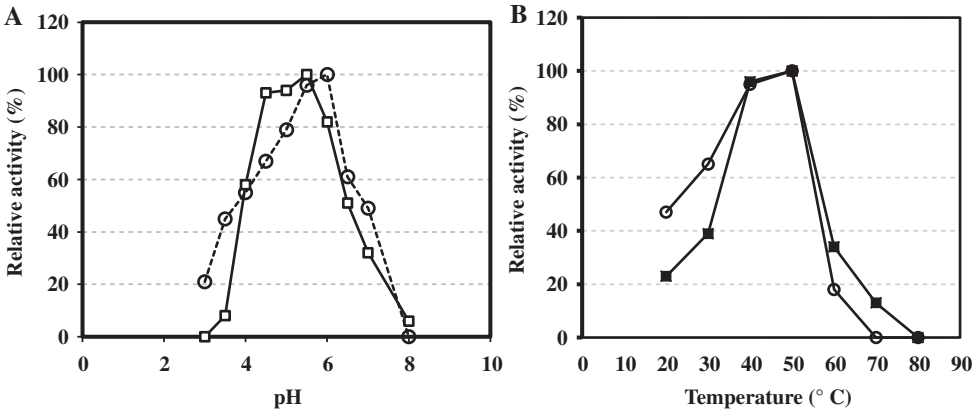

Fig. 5 Effects of pH and temperature on the activity of rMan-Le. (A) The effects of pH on the activity of rMan-Le were examined using M9A and *p*NP-α-Man as substrates at various pH levels (3.0–8.0). The incubation time for natural and synthetic substrates at 37°C were 4 and 1 h, respectively. The buffers used were 0.1 M glycine–HCl (pH 3.0), 0.1 M citrate (pH 3.5–5), 0.1 M MES (pH 5.5–6.5) and 0.1 M HEPES (pH 7.0–8.0). M9A (open square) and *p*NP-α-Man (open circle) Substrate. (B) Effects of temperature on the activity of rMan-Le. Both *p*NP-α-Man and M9A were also used as substrates to analyse the effects of temature on the activity of rMan-Le. Purified rMan-Le (5 µl) was mixed with each of 100 pmol M9A and 100 µmol *p*NP-α-Man in 0.1 M MES buffer, pH 5.5 and incubated at various temperatures (20, 30, 40, 50, 60 70 and 80°C). An incubation times for natural and synthetic substrate were 2 and 1 h, respectively. M9A (open circle) and *p*NP-α-Man (filled square).

Table II. Effects of metals ions and inhibitors on the activity of rMan-Le.

	Percentage of remaining substrate (M9A) and products (M8∼M4) after rMan-Le treatment					
		Products				
Metal ions and inhibitors	M9A remaining	M8	M7	M6	M5	M4
Control	–	2	40	48	8	2
Fe^{2+} (5mM)	10	55	30	5	–	–
Fe^{3+} (5mM)	8	37	42	8	5	–
Co^{2+} (5mM)	–	6	45	38	11	–
Zn^{2+} (5mM)	12	47	35	6	–	–
Cu^{2+} (5mM)	95	5	–	–	–	–
Ca^{2+} (5mM)	8	45	40	7	–	–
Mg^{2+} (5mM)	6	48	40	6	–	–
Mn^{2+-} (5mM)	12	63	25	–	–	–
EDTA (5mM)	8	46	38	8		–
Swainsonine (250 μM)	100	–	–	–		–
DMM (250 μM)	83	17	–	–		–

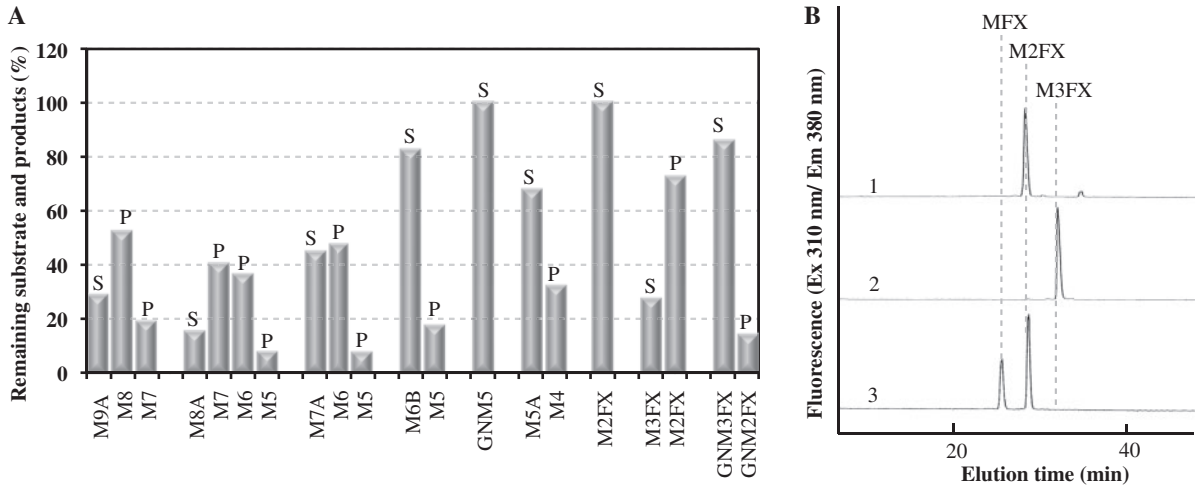

Fig. 6 Substrate specificities and SF-HPLC profile of M3FX treated with rMan-Le. (A) Substrate specificities study. The substrate specificities of rMan-Le were analysed using authentic PA-sugar chains, M9A, M8A, M7B, M6B, GNM5, M5A, M2FX, M3FX and GNM3FX in 0.1 M MES buffer, pH 5.5 at 37°C for 2 h. The PA-sugar chains produced after digestion of rMan-Le were analysed by SF-HPLC on a Shodex Asahipak NH2P-50-4E column (0.46 × 25 cm). S and P are the remaining substrate and products respectively after digestion. M3FX, $Man_3Xyl_1Fuc_1GlcNAc_2$-PA; M2FX, $Man_2Xyl_1Fuc_1GlcNAc_2$-PA; MFX, $ManXyl_1Fuc_1GlcNAc_2$-PA; GN, GlcNAc. (B) SF-HPLC profile of M3FX treated with rMan-Le. M3FX was incubated with purified rMan-Le in 0.1M MES buffer, pH 5.5 at 45°C for 12 h. Products were analysed by SF-HPLC as described bin the text.1 and 2 were undigested M2FX and M3FX, respectively; 3, M3FX treated with purified rMan-Le.

respectively (*38*). Therefore, Man-Le is different from Class II α-mannosidase involved in the *N*-glycan processing in Golgi apparatus. Moreover, the rMan-Le can readily convert M3FX to M2FX but not readily convert M2FX to MFX. Only prolonged incubation (12 h) of M3FX with rMan-Le could produce M2FX (64%) and MFX (36%) (Fig. 6B). On the other hand, 6 h incubation of M5A with rMan-Le could readily produce M3, M2 and M1 products (data not shown). These results suggest that presence of β1-2 Xyl linked to the core β-mannosyl residue hinders the α-mannosidase activity to release α1-3 Man residue from M2FX structure. Therefore, rapid and complete degradation of the plant complex type *N*-glycans must require the concerted reaction of β-*N*-acetylglucosaminidase, β-xylosidase, α-fucosidase and α-mannosidase. Indeed, it has been reported that the truncated plant complex type structure is predominant among *N*-glycans linked to tomato fruit glycoproteins (*39*, *40*). Furthermore, the amount of truncated plant complex type structures ($Man_2Xyl_1Fuc_1GlcNAc_2$, $GlcNAc_1Man_3Xyl_1Fuc_1GlcNAc_2$ and $Man_2Xyl_1GlcNAc_2$) that have the slight resistance to Man-Le accounted for ∼45% of total *N*-glycans of glycoproteins in tomato fruits (*40*), indicating that the release of the α1-3Man in the M2FX structure may have the key to complete turnover of *N*-glycoproteins in mature tomato fruits.

Phylogenetic analysis of Man-Le

The class II α-mannosidases which have been classified under glycosyl hydrolase family 38, can cleave α1-2, α1-3 and α1-6 glycosidic linkages of glycoproteins. They have conserved N-terminal glycosyl hydrolase

superfamily domain, middle α-mannosidase domain and C-terminal glycosyl hydrolase superfamily domain. Enzymes of this class also have a wider range of cellular compartmentalization and can be localized to the cell wall, cytosol, vacuole or lysozyme in addition to Golgi complex. The Man-Le also has such kinds of three consecutive conserved domains in its deduced amino acid sequence. To shed light on the property and evolutionary position of Man-Le, a neighbour-joining phylogenetic tree was constructed (Fig. 7). We used the deduced amino acid sequence of Man-Le as Blastp input to explore the neighbours or homologous sequences. A total of 485 homologous sequences were found to be active hits from GenBank database based on the alignment. For the phylogenetic reconstruction, we included 39 sequences those were previously functionally characterized as α-mannosidases, as well as novel putative α-mannosidases sequences. The resulting neighbour-joining tree suggests that there are three robust clades of acidic α-mannosidases (animals, plants and flies–insects), and plant acidic α-mannosidase originated from ancestral proto-α-mannosidases of amoeba. The Man-Le originated at the final stage of cluster divergence of the tree and very closed to *R. communis* (XP_002511094). Since *Ricinus* (XP_002511094 and XP_002512840), *Arabidopsis* (NP_001031878, BAB11126 and NP_196902), and rice (AB_G22500) putative α-mannosidase genes are relatively closer to Man-Le, these α-mannosidases may have similar substrate specificity and play a similar role in turnover of *N*-glycoproteins in acidic organelle. Phylogenetic analysis suggests that plant acidic α-mannosidase have redundantly evolved, facilitating the efficiency in the turnover of *N*-glycoproteins or *N*-glycans. Such redundant occurrences of acidic α-mannosidase gene suggest that the efficient hydrolysis of α-mannosidic linkage in *N*-glycans must be critical for plant development or growth.

Molecular 3D modelling

3D protein structure is an important source of information to better understand the function of a protein. To study the structure–function relationship, we

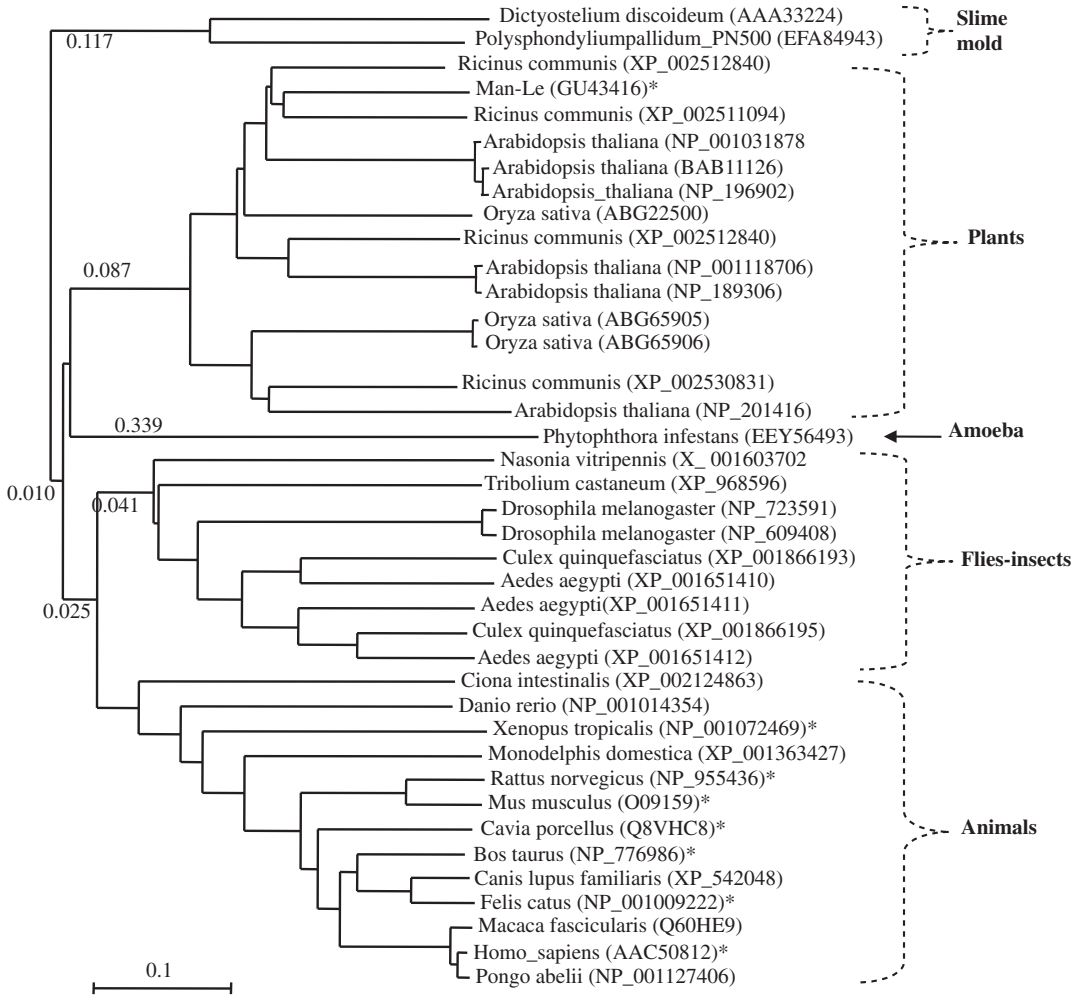

Fig. 7 Neighbour-joining phylogenetic tree analysis of deduced amino acid sequence of acidic α-mannosidase homologues found in NCBI/Blastp search. Multiple sequence alignment was performed using ClustalX (2.0.6) programme. A total of 39 genes those predicted and/or characterized as glycosyl hydrolase super family 38 belong to class II α-mannosidase was taken into consideration for the construction of phylogenetic tree. Asterisk indicated as really characterized α-mannosidase. The analysed α-mannosidases are separated into three main clades in higher eukaryotes: plants, animal and flies–insects. The indicated scale represents 0.1 amino acid substitution per site.

generated a molecular 3D model using X-ray solved bovine lysosomal α-mannosidase (bLAM) (*32*) as template (pdb ID: 1o7d). The average sequence identity of Man-Le with bLAM homologue was 43%. The template alignment mode of the SWISS-MODEL web server was used to solve the modelled-structure. The quality of the modelled-structure was evaluated using structural assessment tools, PROCHECK and WHATIF, which together performed the check on stereo-chemical quality, bond-angle and bond-length, etc. The total QMEAN-score (Composite scoring function for model quality estimation) of solved modelled structure of Man-Le was 0.625 whereas the bLAM had 0.692. The *Z*-score of Man-Le and bLAM were −1.14 and −0.52, respectively. The DFire energy, −1,272.75 was also very close to the template structure, −1,404.75. WHATIF *Z*-score, 1.1 was also good as the expected value of 1.0 for high-quality structure. Most importantly the modelled Man-Le structure had 97.8% of all its residues in conformationally permitted region as predicted by PROCHECK, with 85% being the minimum requirement for high-resolution X-ray crystallographic structure. Only a few residues (0.9%) were in the disallowed region. Therefore, an overall quality of modelled structure was good as checked by both programmes.

An overall structural model of Man-Le is depicted in the Fig. 8A, which included 963 residues with five structural parts, A–E as found in template structure (*32*). An important secondary-structural motif comprised 14 helices and 46 strands. The α and β contents of the model protein were found to be 19.5 and 26.2%, respectively, as predicted by the programme PROMOTIF (Fig. 8A). The modelled Man-Le

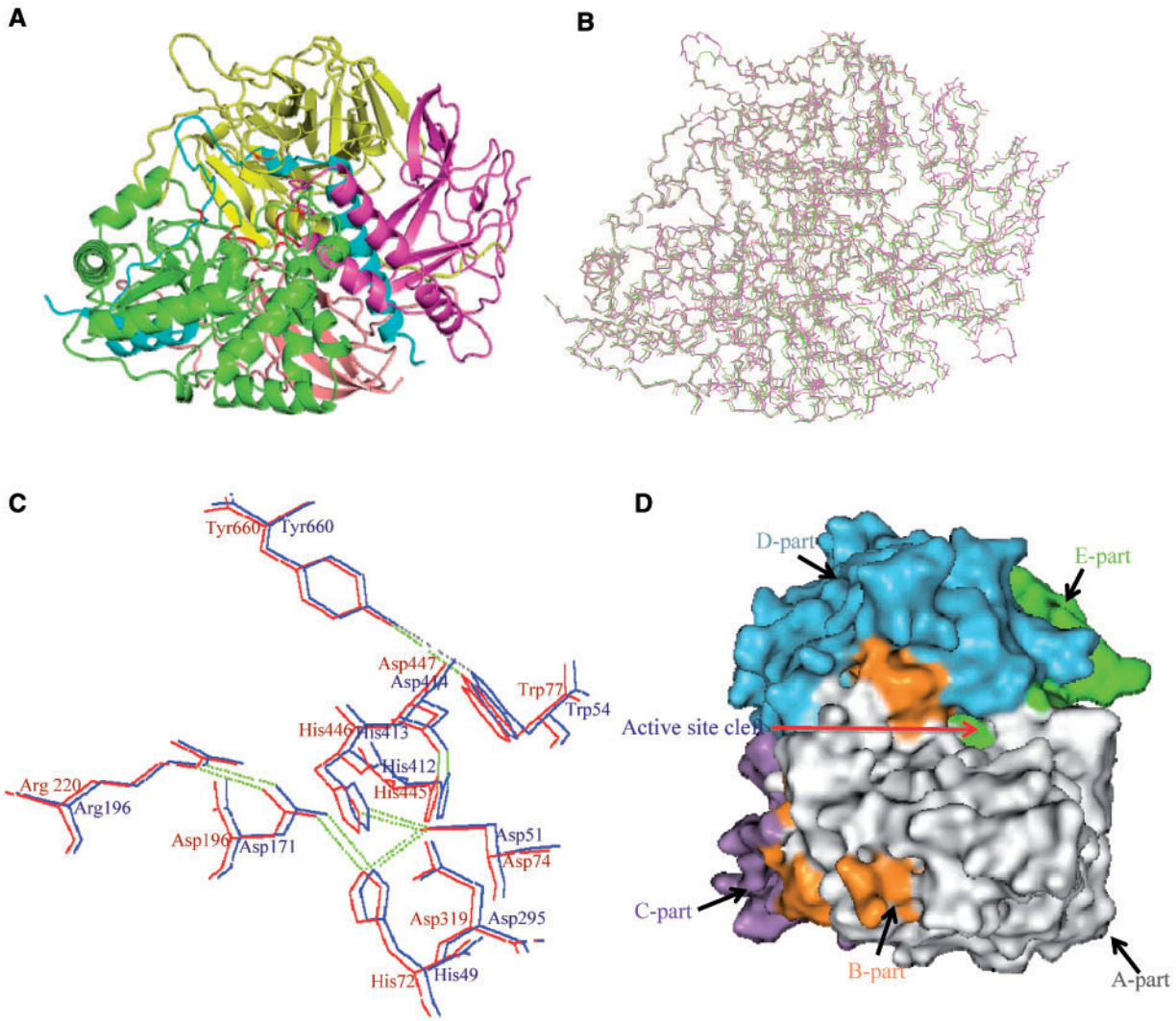

Fig. 8 Molecular 3-D modelling of tomato acidic α-mannosidase solved by SWISS-MODEL web server. (A) The 3D structure contains five polypeptide parts: A-part (green), B-part (cyan), C-part (purple), D-part (yellow) and E-part (pink) as found in crystal structure of bLAM. Locations of the active site amino acid residues (10 aa) are shown in red colour. (B) Modelled 3D structure of Man-Le (purple) was superimposed on the 3D structure of bovine lysosomal α-mannosidase (green). Molecular image were prepared by Polyview-3D and Swiss-PdbViewer. (C) Super imposed image of amino acid residues of located at the active site of modelled structure of Man-Le with X-Ray solved crystal structure of bLAM. Active site residues (10 amino acids) of modelled structure of Man-Le (blue colour) with that of bLAM (purple). (IV) Space filled views of Man-Le structure. A side view of surface filled representation of Man-Le with active site cleft indicated by red arrow. A–E parts are shown in various colour.

structure is composed of four domains; the N-terminal α/β domain, which contains the active site, is formed by the A and B parts. The N-terminal α/β domain is followed by a three-helix bundle joining the B- and C-parts, and three mainly β-sheet domains formed by C–E. There is only one intra-chain disulphide bond in C-part at position Cys469–Cys477 in the structure. Structural similarity was further compared by superimposition of Man-Le homology model template. The modelled structure Man-Le closely resembled the template structure and it had good similarity with the template upon superimposition (Fig. 8B). An amino acid sequence alignment of Man-Le with bLAM showed that 10 amino acids located at the active site of bLAM were conserved in Man-Le (Fig. 3A). The amino acid residues His49, Asp51, Trp54, Asp171, Arg196, Asp295, His412, His413, Asp414 and Tyr660 were estimated as catalytically important residues and also Asp171 was speculated as the corresponding nucleophilic residue. These amino acids are located at the loop region of A-, C- and D-part, which are shown as red colour in the Fig. 8A.

Comparing the superimposition of Cα atoms of Man-Le structure with a crystal model of bLAM reveals that conformation of predicted Man-Le's catalytic site is very similar to the bLAM's catalytic site (Fig. 8C). An active site cleft of modelled structure of Man-Le clearly depicted in the Figure 8D that is also very similar to active site cleft of bLAM (data not shown). The similarity of conserved residues and active site conformation between the modelled structure of Man-Le and bLAM suggests that their catalytic mechanism may be similar to each other. We also used magic fit for superimposition of Man-Le's structure with the crystal structure of dGMII (pdb ID: 3BLB) to compare their structural conformations. The catalytically important amino acids located at the active site of dGMII are His90, Asp92, Trp95, Asp204, Phe206, Tyr269, Arg228, Asp241, His471 and Tyr727. Eight amino acids out of 10 are conserved in Man-Le and therefore, the active site conformation is not well superimposed with dGMII. The four main residues located at the active site cavity of dGMII are Trp95, Phe206, Tyr269 ad Tyr727 (*41*). The last two residues are not conserved in Man-Le, which are replaced by Gly230 and Phe668. Therefore, the catalytic mechanism of plant acidic α-mannosidase may be of somewhat different from that of processing α-mannosidase (dGMII).

Conclusion

In this study, we have successfully cloned and expressed the Man-Le cDNA in *P. pastoris*, and the recombinant enzyme was purified to be homogeneity by anti-Flag affinity column. Like native Man-Le, rMan-Le was inhibited by two α-mannosidase-specific inhibitors, swainsonine and DMM, and showed the optimum activity at weak acidic pH region (pH ~5.5), indicating that Man-Le is slightly different species from typical other plant acidic α-mannosidases [Jack bean (*2*) or rice (*3*)] that showed the optimum activity at rather acidic pH region (pH ~4.5) and were specifically inhibited by swainsonine. Although rMan-Le could hydrolyse α1-2, α1-3, and α1-6 mannosidic linkages in both high-mannose type and truncated complex type *N*-glycans, the presence of β1-2 Xyl residue reduced the hydrolysis rate of α1-3 Man residue in the M2FX structure. Meli *et al.* (*14*) have recently identified a gene encoding one of similar tomato α-mannosidases and proposed that the α-mannosidase and β-hexsosaminidase might be deeply involved in tomato fruit ripening. But the α-mannosidase gene has not been successfully expressed to analyse some biochemical properties including substrate specificity. Since the deduced amino acid sequence of the tomato α-mannosidase (*14*) is slightly different from Man-Le and the substrate specificity or other enzymatic properties are obscure, it is not clear whether Man-Le is the same molecule as the α-mannosidase reported. A molecular 3D model reveals that active site amino acids and conformation of Man-Le are highly conserved with those of bLAM, suggesting that the reaction mechanism must be similar between plant and mammal enzymes working in acidic condition (*32*).

To explore the exact function of free *N*-glycans occurring in developing plant or fruit during ripening, the construction of transgenic tomato plant, in which genes of Man-Le, Endo-LE (*13*) and acidic peptide: *N*-glycanase (PNGase-Le) (*42*) are triple- or double-knocked out or over-expressed, is underway.

Funding

The Ministry of Education, Culture, Sports, Science and Technology of Japan [Basic Research (C), No. 21580414, partial] and Kagome Co. Ltd., partial.

Conflict of interest

None declared.

References

1. Neufeld, E.F. (1991) Lysosomal storage diseases. *Annu. Rev. Biochem. JID – 2985150R* **60**, 257–280
2. Snaith, S.M. (1975) Characterization of jack-bean α-D-mannosidase as zinc metalloenzyme. *Biochem. J.* **147**, 83–90
3. Kishimoto, T., Hori, H., Takano, D., Nakano, Y., Watanabe, M., and Mitsui, T. (2001) Rice α-mannosidase digesting the high mannose glycopeptides of glutelin. *Physiol. Plant* **112**, 15–24
4. Blom, H., Reyes, F., and Carlsson, J. (2008) Purification and characterization of an α-mannosidase from the tropical fruit babaco. *J. Agri. Food Chem.* **56**, 10872–108878
5. Hossain, M.A., Nakamura, K., and Kimura, Y. (2009) α-mannosidase involved in turnover of plant complex type N-glycans in tomato (*Lycopersicum esculentum*) fruits. *Biosci. Biotechnol. Biochem.* **73**, 140–146
6. Priem, B., Gitti, R., Bush, C.A., and Gross, K.C. (1993) Structure of ten free N-glycans in ripening tomato fruits. *Plant Physiol.* **102**, 45–458

7. Priem, B. and Gross, K. (1992) Mannosyl- and xylosyl-containing glycans promote tomato (*Lycopersicon esculentum* Mill.) fruit ripening. *Plant Physiol.* **98**, 399–401
8. Handa, A.K., Sinh, N.K., and Biggs, S.M. (1885) Effect of tunicamycin on in vitro ripening of tomato pericarp tissue. *Physiol. Plant* **63**, 117–121
9. Kimura, Y., Tagaki, S., and Shirai, R.T. (1997) Occurrence of free N-glycans in pea (*Pisum sativum* L) seedlings. *Biosci. Biotechnol. Biochem.* **61**, 924–926
10. Kimura, Y. and Kitahara, E. (2000) Structural analysis of free *N*-glycans occurring in soybean seedlings. *Biosci. Biotechnol. Biochem.* **64**, 2109–2120
11. Kimura, Y. and Matsuo, S. (2000) Free *N*-glycans already occurs at early stage of seed development. *J. Biochem.* **127**, 1013–1019
12. Nakamura, K., Inoue, M., Yoshiie, T., Hosoi, K., and Kimura, Y. (2008) Changes in structural features of free *N*-glycans and endoglycosidase activity during tomato fruit ripening. *Biosci. Biotechnol. Biochem.* **72**, 2936–2945
13. Nakamura, K., Inoue, M., Maeda, M., Nakano, R., Hosoi, K., Fujiyama, K., and Kimura, Y. (2009) Molecular cloning and gene expression analysis of tomato endo-β-*N*-acetylglucosaminidase, an endoglycosidase involved in the production of high-mannose type free N-glycans during tomato fruit ripening. *Biosci. Biotechnol. Biochem.* **73**, 2936–2945
14. Meli, V.S., Ghosh, S., Prabha, T.N., Chakraborty, N., Chakraborty, S., and Datta, A. (2010) Enhancement of fruit shelf life by suppressing N-glycan processing enzymes. *Proc. Natl Acad. Sci. USA* **107**, 2413–2418
15. Tollersrud, O.K., Berg, T., Healy, P., Evjen, G., Ramachandran, U., and Nilssen, Q. (1997) Purification of bovine lysosomal α-mannosidase, characterization of its gene and determination of two mutation that cause α-mannosidosis. *Eur. J. Biocem.* **246**, 410–419
16. Pohlmann, R., Hasilik, A., Cheng, S., Pemble, S., Winchester, B., and Figura, K.V. (1983) Synthesis of lysosomal α-mannosidase in normal and mannosidosis fibroblasts. *Biochem. Biophys. Res. Commun.* **115**, 1083–1089
17. Kimura, Y., Hase, S., Kobayashi, Y., Kyogoku, Y., Ikenaka, T., and Funatsu, G. (1988) Structure of sugar chains of *Ricinus communis* agglutinin. *Biochem. Biophys. Acta* **966**, 248–256
18. Kimura, Y., Hase, S., Ikenaka, T., and Funatsu, G. (1988) Structural analysis of sugar chains from *Abrus precatorius* agglutinin. *Biochem. Biophys. Acta* **966**, 160–167
19. Kimura, Y., Miyagi, C., Kimura, M., Nitoda, T., Kawai, N., and Sugimoto, H. (2000) Structural analysis of *N*-glycans linked to royal jelly glycoproteins. *Biosci. Biotechnol. Biochem.* **64**, 2109–2120
20. Wan, C.Y. and Wilkins, T.A. (1994) A modified hot borate method significantly enhances the yield of high-quality RNA from cotton (*Gossypium hirsutum* L.). *Anal. Biochem.* **223**, 7–12
21. Laemmli, U.K. (1970) Cleavage of structural proteins during the assembly of the head of bacteriophage T4. *Nature* **227**, 680–685
22. Rost, B., Yachdav, G., and Liu, J. (2004) The Predict Protein Server. *Nucleic Acids Res.* **32 (Web Server issue)**, W321–W326
23. Larkin, M.A., Blackshields, G., Brown, N.P., Chenna, R., McGettigan, P.A., McWilliam, H., Valentin, F., Wallace, I.M., Wilm, A., Lopez, R., Thompson, J.D., Gibson, T.J., and Higgins, D.G. (2007) Clustal W and Clustal X version 2.0. *Bioinformatics* **23**, 2947–2948
24. Arnold, K., Bordoli, L., Kopp, J., and Schwede, T. (2006) The SWISS-MODEL Workspace: a web-based environment for protein structure homology modeling. *Bioinformatics* **22**, 195–201
25. Kiefer, F., Arnold, K., Künzli, M., Bordoli, L., and Schwede, T. (2009) The SWISS-MODEL Repository and associated resources. *Nucleic Acids Res.* **37**, D387–D392
26. Schwede, T., Kopp, J., Guex, N., and Peitsch, M.C. (2003) SWISS-MODEL: an automated protein homology-modeling server. *Nucleic Acid Res.* **31**, 3381–3385
27. Zhou, H. and Zhou, Y. (2002) Distance-scaled, finite ideal-gas reference state improves structure-derived potentials of mean force for structure selection and stability prediction. *Protein Sci.* **11**, 2714–2726
28. Benkert, P., Tosatto, S.C.E., and Schomburg, D. (2008) QMEAN: a comprehensive scoring function for model quality assessment. *Proteins: Struct. Funct. Bioinf.* **71**, 261–277
29. Hutchinson, E.G. and Thornton, J.M. (1996) PROMOTIF - a program to identify structural motifs in proteins. *Protein Sci.* **5**, 212–220
30. Laskowski, R.A., MacArthur, M.W., Moss, D., and Thornton, J.M. (1993) PROCHECK: a program to check the stereochemical quality of protein structures. *J. Appl. Cryst.* **26**, 283–291
31. Hooft, W.W., Vriend, G., Sander, C., and Abola, E.E. (1996) Errors in protein structures. *Nature* **381**, 272
32. Heikinheimo, P., Helland, R., Leiros, H-K.S., Leiros, I., Karlsen, S., Evjen, G., Ravelli, R., Schoehn, G., Ruigrok, R., Tollersrud, O-K., McSweeney, S., and Hough, E. (2003) The structure of bovine lysosomal α-mannosidase suggests a novel mechanism for low-pH activation. *J. Mol. Biol.* **327**, 631–644
33. Ogawa, H., Fukumoto, H., Yamamoto, K., Yano, T., and Tochikura, T. (1990) Purification and characterization of α-mannosidase from kiwifruit. *Nippon Shokuhin Kogyo Gakkaishi* **37**, 390–395
34. Nakagawa, H., Enomoto, N., Asakawa, M., and Uda, Y. (1988) Purification and characterization of α-mannosidase and β-acetylhexosaminidase from watermelon fruit. *Agric. Biol. Chem.* **52**, 2223–2230
35. Woo, K.K., Myazaki, M., Hara, S., Kimura, M., and Kimura, Y. (2004) Purification and characterization of a Co (II)-sensitive α-mannosidase from *Gingko biloba* seeds. *Biosci. Biotechnol. Biochem.* **68**, 2547–2556
36. Ohtani, K. and Masaki, A. (1983) Purification and characterization of β- galactosidase and α-mannosidase from papaya (*Carica papaya*) seeds. *Agric. Biol. Chem.* **47**, 2441–2451
37. Petek, F. and Villarrova, E. (1968) Purification and properties of alpha-mannosidase of germinated *Vicia sativa*. *Bull. Soc. Chim. Biol.* **50**, 725–738
38. Strasser, R., Schoberer, J., Jin, C., Glossl, J., Mach, L., and Steikellner, H. (2006) Molecular cloning and characterization of *Arabidopsis thaliana* Golgi α-mannosidase II, a key enzyme in the formation of complex N-glycan in plants. *The Plant J.* **45**, 789–803
39. Zeleney, R., Altman, F., and Praznik, W. (1999) Structural characterization of the N-linked oligosaccharides from tomato fruit. *Phytochemistry* **51**, 199–210
40. Nakamura, K., Inoue, M., Hosoi, K., and Kimura, Y. (2009) Predominant occurrence of truncated complex

type N-glycans among glycoproteins in mature red tomato. *Biosci. Biotechnol. Biochem.* **73**, 221–223
41. Elsen, J.M.H.v.d., Kuntz, D.A., and Rose, D.R. (2001) Structure of Golgi α-mannosidase II: a target for inhibition of growth and metastasis of cancer cells. *The EMBO J.* **20**, 3008–3017
42. Hossain, M.A., Nakano, R., Nakamura, K., and Kimura, Y. (2010) Molecular identification and characterization of an acidic peptide:N-glycanase from tomato (*Lycopersicum esculentum*) fruits. *J. Biochem.* **146**, 157–165